photonics

MDPI

Article

High Concentration Photovoltaics (HCPV) with Diffractive Secondary Optical Elements

Furkan E. Sahin [1,*] and Musa Yılmaz [2]

1 Advanced Research & Development, Maxim Integrated, San Jose, CA 95134, USA
2 Department of Electrical and Electronics Engineering, Batman University, Batman 72060, Turkey; musa.yilmaz@batman.edu.tr
* Correspondence: furkansahin@gmail.com

Received: 5 May 2019; Accepted: 11 June 2019; Published: 12 June 2019

Abstract: Multi-junction solar cells can be economically viable for terrestrial applications when operated under concentrated illuminations. The optimal design of concentrator optics in high concentration photovoltaics (HCPV) systems is crucial for achieving high energy conversion. At a high geometric concentration, chromatic aberration of the primary lens can restrict the optical efficiency and acceptance angle. In order to correct chromatic aberration, multi-material, multi-element refractive elements, hybrid refractive/diffractive elements, or multi-element refractive and diffractive systems can be designed. In this paper, the effect of introducing a diffractive surface in the optical path is analyzed. An example two-stage refractive and diffractive optical system is shown to have an optical efficiency of up to 0.87, and an acceptance angle of up to $\pm 0.55°$ with a $1600\times$ geometric concentration ratio, which is a significant improvement compared to a single-stage concentrator system with a single material. This optical design can be mass-produced with conventional fabrication methods, thus providing a low-cost alternative to other approaches, and the design approach can be generalized to many other solar concentrator systems with different cell sizes and geometric concentration ratios.

Keywords: high concentration photovoltaics; diffractive optics; optical system design; solar energy; Fresnel lens; secondary optical element

1. Introduction

Multi-junction solar cells have been traditionally used in space applications, and are now gaining popularity in terrestrial photovoltaics (PV) [1–3]. These devices stack multiple bandgap units (typically 3 or 4) to provide high-efficiency energy conversion over the broadband solar spectrum (Figure 1). Due to their complex, multilayer structure and the choice of different semiconductor materials, multi-junction cells are expensive when compared to silicon PV cells. The active solar cell area can be reduced with the help of low-cost concentrator optics, and the overall system cost can thus be lowered with minimal effect on performance. Among concentrated photovoltaics (CPV) systems, concentration levels higher than $400\times$ are typically considered high concentration photovoltaics (HCPV) [4]. In addition to the level of concentration, the acceptance angle of a CPV system is also a critical parameter. The sun subtends to an angle of about $\pm 0.25°$ in the sky, meaning that a solar concentrator system should have an acceptance angle that matches and exceeds this value. Most CPV systems have very limited acceptance angles, and therefore require tracking and orientation systems to keep the sun in the field of view [5–7]. Increasing acceptance angles of concentrator optics will result in reduced alignment accuracy and tracking requirements, lowering the overall cost of the system. The concentrator system should itself be of low cost, and made out of commonly available materials through mass-production methods. A simple solar concentrator system can be constructed with either a reflective (mirror) or a refractive (lens) primary optical element (POE). Refractive POEs (e.g., Fresnel lenses) are typically preferred, because they are more tolerant to manufacturing errors than mirrors [8]. At high concentration ratios, optical aberrations (such as spherical and chromatic aberration) of the POE limit the optical efficiency and acceptance angle of the system.

The sun is a broadband energy source, with the useful spectrum being from 380 nm to 1.6 µm, as shown in Figure 1. A solar CPV concentrator system should be designed such that the wavelengths of light in this range are focused onto the solar cell. This can be achieved through designing a chromatic aberration-corrected (achromatized) optical concentrator system. Spherical aberration of the POE can be minimized by designing a Fresnel lens with an optimized aspherical surface profile. Refractive concentrators are typically rotationally symmetric, and due to the narrow acceptance angles, other monochromatic optical aberrations, such as the coma or distortion, are not pronounced [9,10]. Chromatic aberration can be minimized through a doublet element (with two different optical materials) or a hybrid refractive/diffractive design approach for the POE [11,12]. Another option would be to introduce a secondary optical element (SOE), typically placed on the solar cell, in addition to the POE [13,14].

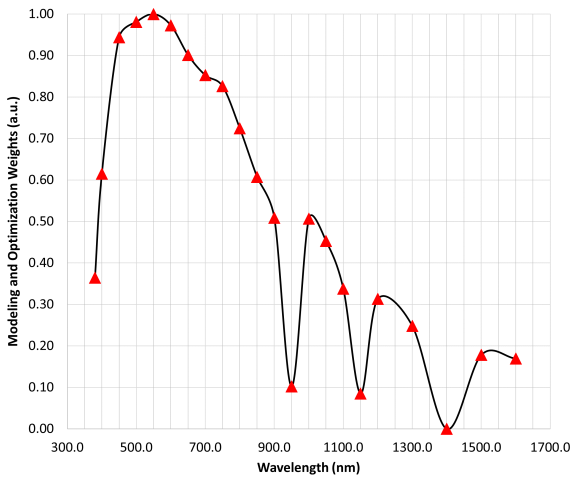

Figure 1. Solar spectrum in the visible and near-infrared regions. Relative weights for wavelengths used in the optimization and analyses are shown with the red triangles [15].

In this paper, a novel concept for achromatization through the optical design of a diffractive secondary optical element is presented, and this is shown to both increase optical efficiency, widen acceptance angles, and loosen assembly tolerances. There are several advantages of implementing a diffractive SOE. In the case of a hybrid refractive/diffractive lens (in which the diffractive surface is on the refractive Fresnel primary optical element), the full area of the POE should have a diffractive profile. This means the large-area Fresnel lens needs to have diffractive features on the order of 1 µm, and this can be challenging to fabricate. When placed on the solar cell as an SOE, the diffractive element can be made smaller, and therefore be easier to fabricate. Compared to refractive SOEs, a diffractive SOE will be planar and thin. The multi-junction solar cell is already packaged in an optically clear and robust package, with either a coverglass or an overmolded optical plastic. The diffractive SOE can be etched directly onto the coverglass or replicated onto the overmolded plastic material. The unique contributions of this paper are:

(a) A design approach for a two-stage photovoltaic concentrator system, with a refractive primary optical element and a diffractive secondary optical element.
(b) An evaluation of the distance between the diffractive surface and the solar cell plane, and its effect on the system parameters.
(c) An optimized refractive–diffractive design that has a 1600× geometric concentration ratio, on-axis optical efficiency of 0.87, and acceptance angle of ±0.55°.

2. Optical Concentrator Systems for Concentrated Photovoltaics

Solar concentration for photovoltaics is typically achieved with a refractive optical system, using a Fresnel lens as the POE . The light incident on the Fresnel lens is focused onto a tight focal point, and the small solar cell is placed at this focus. Fresnel lenses can be mass-produced at a low cost out of optical plastics (e.g., polymethylmethacrylate (PMMA), polycarbonate) with replication methods [16]. PMMA is commonly used in solar applications, and available from various manufacturers under different trade names, such as Plexiglas, Lucite, or Acrylite. The unique advantage of PMMA for CPV applications is its low transmission in infrared wavelengths, and therefore its potential to reduce excess heating [17]. Fresnel lenses can also be replicated on silicone attached to a flat glass plate, an approach known as Silicone-on-Glass (SoG) [18]. The geometric concentration ratio C_{geo} and optical efficiency η_{opt} are two parameters that characterize the collection in a solar concentrator. The geometric concentration ratio is the ratio between the collector (i.e., Fresnel lens) area ($A_{collector}$) and the solar cell receiver area ($A_{receiver}$). Optical efficiency is the ratio between the optical power incident on the receiver ($\Phi_{receiver}$) and the optical power incident on the collector ($\Phi_{collector}$) [19].

$$C_{geo} = \frac{A_{collector}}{A_{receiver}}, \tag{1}$$

$$\eta_{opt} = \frac{\Phi_{receiver}}{\Phi_{collector}}, \tag{2}$$

$$C_{opt} = \frac{(\Phi_{receiver}/A_{receiver})}{(\Phi_{collector}/A_{collector})} = \eta_{opt} C_{geo}. \tag{3}$$

The purpose of the CPV system is to concentrate the power incident on the collector onto a small receiver area. The optical concentration ratio C_{opt} is the ratio between the power per area at the collector and at the receiver [19].

If all the optical power that is incident on the collector is also incident on the receiver (i.e., $\eta_{opt} = 1$), then the power per area is concentrated by the geometric concentration ratio C_{geo}. However, for a given collector-receiver pair, not all rays incident on the collector will make it to the receiver. Optical aberrations, Fresnel reflections at material–air interfaces, and transmission losses through optical materials limit the total power from reaching the receiver, resulting in a reduced η_{opt}.

Fresnel reflections occur at interfaces with different refractive indices on either side. For a typical optical material ($n = 1.5$) to air ($n = 1$) interface, at a normal incidence of light, 4% of optical power is not transmitted due to the Fresnel reflection. Assuming the solar cell is enclosed in an index-matched coverglass (or an SOE), a typical CPV system with uncoated surfaces will have three air–material interfaces (two interfaces for POE and one for the receiver), with about 12% total loss due to Fresnel reflections. Anti-reflection (AR) coatings can be applied to each of the optical surfaces to minimize this Fresnel loss. These AR coatings should be broadband ones to cover the full useful spectrum of the sun (380 nm to 1.6 µm) [20]. In order to minimize transmission losses, high-transmittance (low-absorption) optical materials should be selected for both the POE and the SOE design, and these components should be made as thin as possible.

3. Chromatic Aberration

Chromatic aberration results from the dispersive nature of optical materials; that is, the material's refractive index (n) changes with wavelength. The refractive index of PMMA varies from 1.511 at 380 nm to 1.480 at 1.6 µm. This means short wavelengths are refracted more than long wavelengths. The Abbe number (V) for an optical material shows how dispersive a material is, and is defined as:

$$\text{Abbe number:} = \frac{n_{center} - 1}{n_{short} - n_{long}}. \tag{4}$$

The Abbe number is typically defined for the visible spectrum, for which n_{center}, n_{short} and n_{long} are the refractive indices of the material at 588 nm, 486 nm, and 656 nm, respectively (Fraunhofer d, F, and C lines). For the case of solar concentrators, which cover a wider range of wavelengths including near-infrared, a solar Abbe number can be defined [21]. Selecting 990 nm, 380 nm, and 1.6 µm for the center, short, and long wavelengths, the solar Abbe number for the PMMA is 15.92.

Two commonly utilized techniques for chromatic aberration correction (achromatization) are refractive and diffractive correction.

3.1. Refractive Achromatization

A traditional method for chromatic aberration correction is to design a multi-element lens with different optical materials. A doublet with a low-dispersion (high Abbe number) positive lens and a high-dispersion (low Abbe number) negative lens can be designed to bring two wavelengths of light to the same focus. These two lenses can be in contact or have some air separation. In the context of solar concentrators, Fresnel doublets have been designed for achromatization of the POE. One example is a low-dispersion PMMA and high-dispersion PC (polycarbonate) doublet Fresnel lens by Languy et al. [12]. Another approach has been an achromatic doublet on glass lens designed by Askins et al., where a low-dispersion elastomer was coupled with high-dispersion plastic (PC) [22]. One advantage of these approaches is that they provide chromatic correction of the POE lens, and thus eliminate the need for an SOE to achieve achromatization. However, making the POE more complex requires sophisticated fabrication methods, and can increase the overall cost of the system.

3.2. Diffractive Achromatization

In addition to refractive lenses, diffractive elements are also widely used in optical system design. These lenses have features on the order of the wavelength, and rely on diffraction and interference for ray bending. They are commonly used in optical systems for spectral-splitting and beam-shaping applications [23], in addition to chromatic aberration correction in lens design [24]. Instead of combining multiple refractive lens elements with different Abbe numbers, a diffractive element can be introduced for achromatization. The dispersive property of a diffractive element depends on the wavelength, but not on the material refractive index. An equivalent diffractive Abbe number for a diffractive element can be defined as [25]:

$$\text{Diffractive Abbe number: } = \frac{\lambda_{center}}{\lambda_{short} - \lambda_{long}}. \tag{5}$$

The diffractive Abbe number is always negative, meaning that chromatic correction can thus be achieved through combining a diffractive surface with a refractive element. Considering the solar spectrum wavelengths ($\lambda_{center} = 990$ nm, $\lambda_{short} = 380$ nm, and $\lambda_{long} = 1.6$ µm), the equivalent Abbe number for a diffractive element is -0.811. There have been approaches for chromatic aberration correction with a hybrid refractive/diffractive optical design approach. In this case, a diffractive surface is added to the front surface of the POE Fresnel lens, which is typically flat to begin with [8,11].

4. Design Approach

In this study, a diffractive optical element (DOE) was placed on the solar cell to achieve chromatic correction, and therefore increase optical efficiency and the acceptance angle, and reduce assembly tolerance requirements.

The primary optical element is a circular Fresnel lens with a diameter of 400 mm, and the receiver is a circular solar cell with a diameter of 10 mm. The corresponding geometric concentration ratio is 1600×. A schematic drawing of the system is shown in Figure 2. This is a representative example, and the same approach can be scaled to different Fresnel lens and solar cell dimensions.

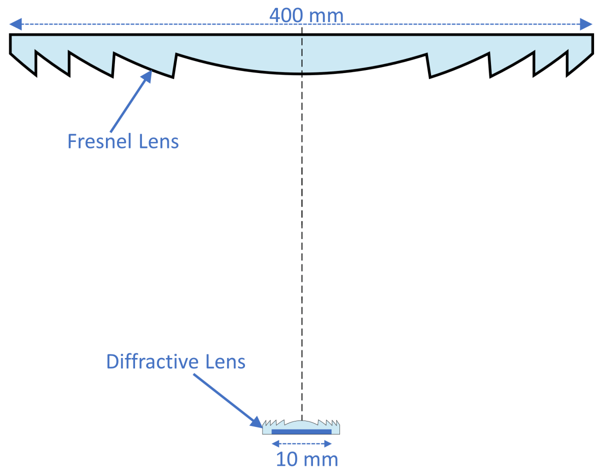

Figure 2. Schematic drawing of the designed high-concentration photovoltaics (HCPV) system with a diffractive secondary optical element. (Not drawn to scale).

Initially, the POE Fresnel lens was designed and optimized without an SOE. The POE had an aspherical surface to minimize the spherical aberration in the system. The total length of the optical system was constrained to be less than 45 cm for all designs. This corresponds to a $f/number$ of about $f/1.1$. In modeling and system optimization, the broadband solar spectrum (as shown in Figure 1) was used. In addition to the POE-only design, three two-stage systems were also designed. Three different thickness values for the diffractive SOE were considered—2 mm, 5 mm, and 10 mm, with diameters of 12.8 mm, 17 mm, and 24 mm, respectively. The diameter of the diffractive SOE was scaled such that the rays concentrated by the POE could be collected by the SOE. As the goal of placing the diffractive surface on the solar cell was to have a small diffractive element for easier fabrication, an SOE thickness of up to 10 mm was considered with a corresponding diameter of 24 mm. For each of these SOE designs, the POE surface was also re-optimized to achieve system level performance improvements. In each case, the solar cell was assumed to be embedded inside the SOE, to minimize index mismatch. The concentrator optical system was initially designed with sequential mode in OpticStudio (Zemax), which allowed for efficient and quick optimization. Once a satisfactory design was reached, it was analyzed in non-sequential mode in OpticStudio [26]. Non-sequential ray-tracing allows for simulation of effects such as Fresnel reflections at surfaces. During system optimization, the minimum zone width for the diffractive element was constrained to be greater than 1.4 µm. Typically, the zone depth of the diffractive profile is twice that of the wavelength, and setting a minimum zone width constraint ensures an aspect ratio of about 1:1, to ensure manufacturability. Sub-micron features have been demonstrated with glass etching or replication of optical plastics [27–29]. The POE lens was modeled as an ideal refractive Fresnel lens, and this is a valid approximation for lenses with fine grooves. Physical Fresnel lenses have inactive faces which reduce light-gathering efficiency. The SOE was modeled as an ideal diffractive element. In this case, the phase change across the lens surface is continuous; therefore, real diffractive elements with discrete steps (such as those manufactured on glass through lithography and etching) will have some deviation from the ideal model described herein.

5. Results

CPV systems are usually designed to have maximum optical efficiency with normal incidence, and efficiency rolls off with the light incidence angle. At high concentration levels, such as the 1600× geometric concentration ratio presented in this paper, chromatic aberration of the POE will limit the optical efficiency for the normal incidence of light (on-axis). With the introduction of a diffractive SOE, on-axis optical efficiency can be increased from 0.79 to 0.85, as shown in Figure 3 and listed in Table 1. By increasing the thickness of the SOE, on-axis optical efficiency can be further increased to

0.87. Considering the Fresnel losses at three air–material interfaces, an optical efficiency level of 0.87 is close to the theoretical maximum value.

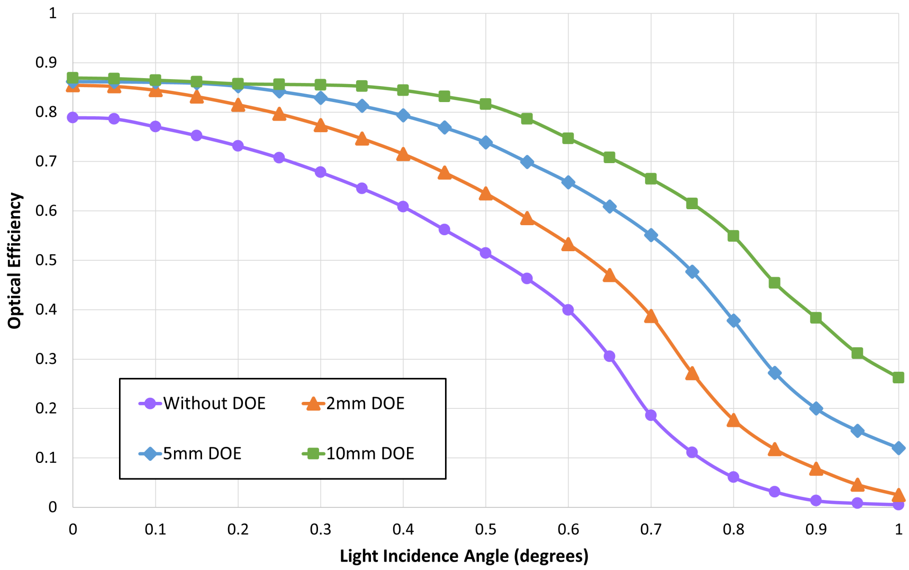

Figure 3. Angular efficiency curves for the different optical configurations studied. DOE: diffractive optical element.

In order to analyze the acceptance angle of the various designs, the angular efficiency curves were generated (Figure 3). Angles corresponding to relative light transmission levels of 90%, 80%, and 50% (α_{90}, α_{80} and α_{50}, respectively) of the maximum achieved with normal incidence were obtained from the angular efficiency plot. Typically, the α_{90} value is quoted as the acceptance angle [30].

Table 1. Optical efficiency (normal incidence) for the different optical designs presented. α_{90}, α_{80}, and α_{50} are the light incidence angles corresponding to 90%, 80%, and 50% of the maximum optical efficiency. SOE: secondary optical element.

SOE	Optical Efficiency	α_{90}	α_{80}	α_{50}
Without DOE	0.79	±0.23°	±0.36°	±0.60°
2 mm thick DOE	0.85	±0.31°	±0.45°	±0.68°
5 mm thick DOE	0.86	±0.44°	±0.57°	±0.78°
10 mm thick DOE	0.87	±0.55°	±0.67°	±0.86°

As shown in Figure 3, the optical efficiency and acceptance angle increase as the SOE is made thicker. In this case, the second (flat) surface of the diffractive SOE is assumed to be in contact with the solar cell for all designs (to minimize Fresnel losses). Therefore, increasing the element thickness effectively increases the distance between the diffractive surface and the solar cell. Due to the chromatic aberration of the POE, incoming light is significantly dispersed by the time it reaches the diffractive surface, a sufficient optical path is required after the diffractive surface to achieve a chromatically-corrected, tight spot at the solar cell plane. As the thickness of the SOE is increased, the diameter should also grow proportionally, increasing the number of diffractive zones. In order to keep a compact and easily manufacturable DOE design, thickness values of up to 10 mm are considered. The design with a 10 mm thick diffractive SOE has the largest acceptance angle of ±0.55°. This is about twice the angular size of the sun, which is a significant improvement compared to the case without a diffractive surface, for which the acceptance angle is only ±0.23°.

The results shown in Figure 3 and listed in Table 1 are for the nominal assembly of the solar concentrator system. However, assembly equipment have limited alignment accuracy, and there could be cases of misalignment. One method to prevent misalignment could be to use active alignment of the solar cell and the SOE [31,32]; however, this makes the assembly procedure more complex, and increases costs. In order to analyze how misalignment could impact both the optical efficiency and acceptance angle, the case of 2 mm misalignment between the Fresnel lens and the diffractive SOE was simulated. As shown in Figure 4, with this misalignment, the optical efficiency for designs without DOE drops from 0.79 to 0.73, whereas for the 10 mm thick diffractive SOE design, the drop is negligible. In addition, the acceptance angle of the design without DOE drops to $\pm 0.13°$, whereas the acceptance angle for the 10 mm thick diffractive SOE design is $\pm 0.38°$. Thus, we can conclude that incorporating a suitable diffractive SOE makes the concentrator design less sensitive to assembly tolerances.

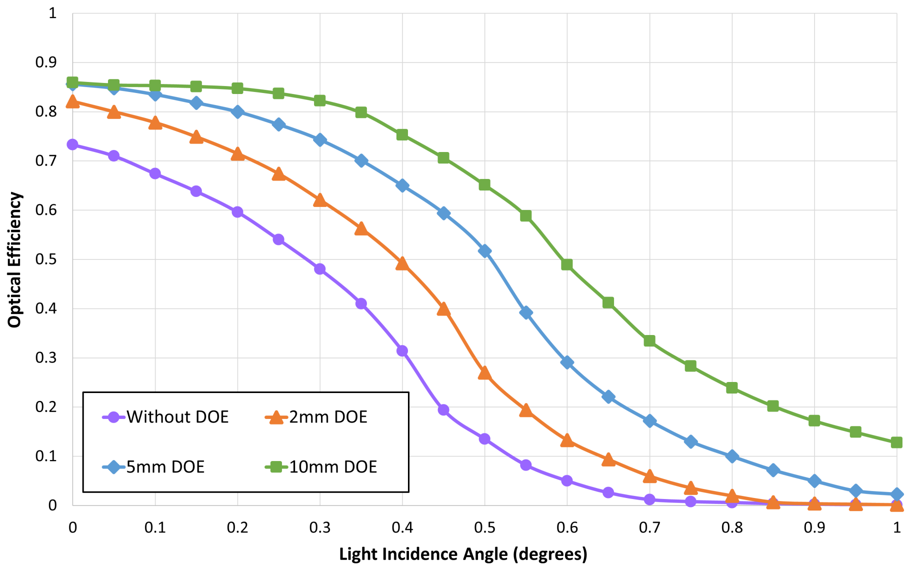

Figure 4. Angular efficiency curves for the different optical configurations studied, with 2 mm misalignment between the Fresnel lens and the diffractive SOE.

6. Discussion

In this paper, geometrical optical design and evaluation of a solar concentrator system was studied. In order to prove the concept, an example case of a circular Fresnel lens (POE), a circular diffractive lens (SOE), and a circular solar cell was assumed. However, concentrator POEs and solar cells can be rectangular in shape. Without loss of generality, the same design principles can be applied to different shapes. In optical modeling, PMMA is considered as the material of POE and SOE. However, as explained above, the diffractive optical element is not related to the material. The same diffractive structure can be made out of other optical plastics or glasses. The diffractive surface is modeled as a continuous phase change. The rotationally symmetric variation of the diffraction-grating period can then be derived from this phase profile. If the manufacturing steps of the diffractive element require discrete binary steps (such as those fabricated through photolithography and etching), efficiency of the diffractive element will be less than that predicted by the ideal model [33]. In this paper, commercial software based on geometric optics was utilized to design a refractive and diffractive solar concentrator system. In order to achieve more accurate results, specialized software tools for the modeling of diffractive optical elements (such as those based on rigorous coupled-wave analysis) can be used.

7. Conclusions

With their high energy-conversion efficiency, multi-junction solar cells are promising candidates for the widespread adoption of photovoltaic systems. In order to make them economically viable, these multi-junction cells are typically operated under concentrated sunlight. With high levels of geometrical concentration, aberrations of the concentrator optics may limit the optical efficiency and acceptance angle. As the sun has a broad spectrum, chromatic aberration is a major reason for reduced efficiency. In this paper, the optical design of a two-stage optical concentrator system was presented. The primary optical element is a Fresnel lens with an optimized aspherical surface profile. As a unique approach, the secondary optical element was a planar element with a diffractive surface. The combined system was optimized to have minimal spherical and chromatic aberration; that is, all wavelengths of sunlight were brought to a common focus on the solar cell. With this approach, the concentrator system has increased optical efficiency, a widened acceptance angle, and reduced tolerance sensitivity compared to a simple single-stage system. The thickness of the diffractive element (i.e., the distance between the diffractive surface and the solar cell plane) is an important factor in design optimization. A design with a diffractive element that is 10 mm thick was shown to have an optical efficiency of 0.87 and an acceptance angle of $\pm 0.55°$ for nominal operation.

Author Contributions: Conceptualization, F.E.S. and M.Y.; Methodology, F.E.S.; Software, F.E.S.; Validation, F.E.S. and M.Y.; Formal Analysis, F.E.S.; Investigation, F.E.S. and M.Y.; Writing, F.E.S. and M.Y.

Funding: This research received no external funding.

Conflicts of Interest: The authors declare no conflict of interest.

References

1. King, R.R.; Fetzer, C.M.; Law, D.C.; Edmondson, K.M.; Yoon, H.; Kinsey, G.S.; Krut, D.D.; Ermer, J.H.; Hebert, P.; Cavicchi, B.T.; et al. Advanced III-V multijunction cells for space. In Proceedings of the 2006 IEEE 4th World Conference on Photovoltaic Energy Conference, Waikoloa, HI, USA, 7–12 May 2006; Volume 2, pp. 1757–1762.
2. Law, D.C.; King, R.; Yoon, H.; Archer, M.; Boca, A.; Fetzer, C.; Mesropian, S.; Isshiki, T.; Haddad, M.; Edmondson, K.; et al. Future technology pathways of terrestrial III–V multijunction solar cells for concentrator photovoltaic systems. *Sol. Energy Mater. Sol. Cells* **2010**, *94*, 1314–1318. [CrossRef]
3. Shvarts, M.Z.; Gudovskikh, A.S.; Kalyuzhnyy, N.A.; Mintairov, S.A.; Mintairov, M.A.; Nakhimovich, M.V.; Emelyanov, V.M. Current localization in heterostructures of multijunction solar cells: Causes for arising and diagnostics potential. *AIP Conf. Proc.* **2018**, *2012*, 040010. [CrossRef]
4. Kurtz, S. *Opportunities and Challenges for Development of a Mature Concentrating Photovoltaic Power Industry (Revision)*; Technical Report; National Renewable Energy Laboratory (NREL): Golden, CO, USA, 2012.
5. Sumathi, V.; Jayapragash, R.; Bakshi, A.; Akella, P.K. Solar tracking methods to maximize PV system output—A review of the methods adopted in recent decade. *Renew. Sustain. Energy Rev.* **2017**, *74*, 130–138. [CrossRef]
6. Mousazadeh, H.; Keyhani, A.; Javadi, A.; Mobli, H.; Abrinia, K.; Sharifi, A. A review of principle and sun-tracking methods for maximizing solar systems output. *Renew. Sustain. Energy Rev.* **2009**, *13*, 1800–1818. [CrossRef]
7. Sahin, F.E. Fisheye lens design for sun tracking cameras and photovoltaic energy systems. *J. Photonics Energy* **2018**, *8*, 035501. [CrossRef]
8. Languy, F. Achromatization of Nonimaging Fresnel Lenses for Photovoltaic Solar Concentration Using Refractive and Diffractive Patterns. Ph.D. Thesis, Université de Liège, Lège, Belgique, 2012.
9. Fischer, R.E. *Optical System Design*; McGraw Hill: New York, NY, USA, 2000.
10. Sahin, F.E.; Tanguay, A.R. Distortion optimization for wide-angle computational cameras. *Opt. Express* **2018**, *26*, 5478–5487. [CrossRef]
11. Languy, F.; Lenaerts, C.; Loicq, J.; Habraken, S. Achromatization of solar concentrator thanks to diffractive optics. In Proceedings of the 2nd International Workshop on Concentrating Photovoltaic Optics and Power, Darmstadt, Germany, 9–10 March 2009.
12. Languy, F.; Fleury, K.; Lenaerts, C.; Loicq, J.; Regaert, D.; Thibert, T.; Habraken, S. Flat Fresnel doublets made of PMMA and PC: Combining low cost production and very high concentration ratio for CPV. *Opt. Express* **2011**, *19*, A280–A294. [CrossRef] [PubMed]
13. Victoria, M.; Domínguez, C.; Antón, I.; Sala, G. Comparative analysis of different secondary optical elements for aspheric primary lenses. *Opt. Express* **2009**, *17*, 6487–6492. [CrossRef] [PubMed]

14. Schmid, T.; Wiesenfarth, M.; Hornung, T.; Gremmelspacher, M.; Manns, P.; Nitz, P. Mass manufactured secondary optics for CPV. *AIP Conf. Proc.* **2014**, *1616*, 84–87.
15. G03 Committee. *Tables for Reference Solar Spectral Irradiances: Direct Normal and Hemispherical on 37° Tilted Surface*; ASTM International: West Conshohocken, PA, USA, 2012.
16. Xie, W.; Dai, Y.; Wang, R.; Sumathy, K. Concentrated solar energy applications using Fresnel lenses: A review. *Renew. Sustain. Energy Rev.* **2011**, *15*, 2588–2606. [CrossRef]
17. Micheli, L.; Sarmah, N.; Luo, X.; Reddy, K.; Mallick, T.K. Infrared reflecting coverglasses for multijunction cells in a terrestrial high-concentrating photovoltaic system. In Proceedings of the 27th European Photovoltaic Solar Energy Conference and Exhibition, Frankfurt, Germany, 24–28 September 2012.
18. Steiner, M.; Bösch, A.; Dilger, A.; Dimroth, F.; Dörsam, T.; Muller, M.; Hornung, T.; Siefer, G.; Wiesenfarth, M.; Bett, A.W. FLATCON® CPV module with 36.7% efficiency equipped with four-junction solar cells. *Prog. Photovolt. Res. Appl.* **2015**, *23*, 1323–1329. [CrossRef]
19. Leutz, R.; Suzuki, A. *Nonimaging Fresnel Lenses: Design and Performance of Solar Concentrators*; Springer Series in Optical Sciences; Springer: Berlin/Heidelberg, Germany, 2012; Chapter 2, pp. 15–34.
20. Young, N.; Perl, E.; Farrell, R.; Iza, M.; Keller, S.; Bowers, J.; Nakamura, S.; DenBaars, S.; Speck, J. High-performance broadband optical coatings on InGaN/GaN solar cells for multijunction device integration. *Appl. Phys. Lett.* **2014**, *104*, 163902. [CrossRef]
21. Vallerotto, G.; Victoria, M.; Askins, S.; Herrero, R.; Domínguez, C.; Antón, I.; Sala, G. Design and modeling of a cost-effective achromatic Fresnel lens for concentrating photovoltaics. *Opt. Express* **2016**, *24*, A1245–A1256. [CrossRef] [PubMed]
22. Askins, S.; Vallerotto, G.; Victoria, M.; Herrero, R.; Domínguez, C.; Antón, I.; Sala, G. A manufacturable achromatic fresnel lens for CPV. In Proceedings of the 2016 IEEE 43rd Photovoltaic Specialists Conference (PVSC), Portland, OR, USA, 5–10 June 2016; pp. 204–209.
23. Miklyaev, Y.V.; Imgrunt, W.; Pavelyev, V.S.; Kachalov, D.G.; Bizjak, T.; Aschke, L.; Lissotschenko, V.N. Novel continuously shaped diffractive optical elements enable high efficiency beam shaping. In Proceedings of the International Society for Optics and Photonics, San Jose, CA, USA, 3 March 2010; Optical Microlithography XXIII; Volume 7640, p. 764024.
24. Sahin, F.E. Design of Hybrid Refractive/Diffractive Lenses for Wearable Reality Displays. *Balk. J. Electr. Comput. Eng.* **2019**, *7*, 94–98. [CrossRef]
25. Schaub, M.; Schwiegerling, J.; Fest, E.; Shepard, R.; Symmons, A. *Molded Optics: Design and Manufacture*; Series in Optics and Optoelectronics; CRC Press: Boca Raton, FL, USA, 2016; pp. 28–32.
26. Zemax LLC. *OpticStudio User Manual*; Zemax LLC: Kirkland, WA, USA, 2017.
27. Roeder, M.; Schilling, P.; Hera, D.; Guenther, T.; Zimmermann, A. Influences on the fabrication of diffractive optical elements by injection compression molding. *J. Manuf. Mater. Process.* **2018**, *2*, 5. [CrossRef]
28. Kalima, V.; Pietarinen, J.; Siitonen, S.; Immonen, J.; Suvanto, M.; Kuittinen, M.; Mönkkönen, K.; Pakkanen, T. Transparent thermoplastics: Replication of diffractive optical elements using micro-injection molding. *Opt. Mater.* **2007**, *30*, 285–291. [CrossRef]
29. Mohammad, N.; Meem, M.; Shen, B.; Wang, P.; Menon, R. Broadband imaging with one planar diffractive lens. *Sci. Rep.* **2018**, *8*, 2799. [CrossRef] [PubMed]
30. Wang, C.M.; Huang, H.I.; Pan, J.; Kuo, H.Z.; Hong, H.F.; Shin, H.Y.; Chang, J.Y. Single stage transmission type broadband solar concentrator. *Opt. Express* **2010**, *18*, A118–A125. [CrossRef] [PubMed]
31. Karp, J.H.; Tremblay, E.J.; Ford, J.E. Planar micro-optic solar concentrator. *Opt. Express* **2010**, *18*, 1122–1133. [CrossRef] [PubMed]
32. Sahin, F.E. Lens design for active alignment of mobile phone cameras. *Opt. Eng.* **2017**, *56*, 065102. [CrossRef]
33. Kim, N.H. *How Diffractive Surfaces Are Modeled in OpticStudio*; Zemax: Kirkland, WA, USA, 2018.